

Spectroscopic Evidence for *Intermolecular* M–H···H–OR Hydrogen Bonding: Interaction of WH(CO)₂(NO)L₂ Hydrides with Acidic Alcohols

Elena S. Shubina,[†] Natalia V. Belkova,[†] Aleksandr N. Krylov,[†]
Evgeni V. Vorontsov,[†] Lina M. Epstein,^{*,†} Dmitri G. Gusev,[‡]
Martina Niedermann,[‡] and Heinz Berke^{*,‡}

Contribution from the Institute of Organo-Element Compounds, Russian Academy of Sciences, Vavilov Str. 28, Moscow B-334, Russia, and Anorganisch-Chemisches Institut, Universität Zürich, Winterthurerstr. 190 CH-8057 Zurich, Switzerland

Received September 7, 1995[⊗]

Abstract: *Intermolecular* hydrogen bonding of acidic alcohols (PhOH, (CF₃)₂CHOH (HFIP), (CF₃)₃CHOH (PFTB)) to the hydride ligand of WH(CO)₂(NO)L₂ (L = PMe₃ (**1**), PEt₃ (**2**), P(OⁱPr)₃ (**3**), PPh₃ (**4**)) has been observed and characterized by IR and NMR spectroscopy in hexane, toluene-*d*₈, and CD₂Cl₂ solutions. The H-bonding is an equilibrium process with medium $-\Delta H^\circ$ of 4.1–6.9 kcal/mol; the enthalpy increases on going from **4** to **1**, i.e., the strongest bonding is found for the smallest and the most basic L = PMe₃. The value of $-\Delta H^\circ$ depends on the pK_a of the proton donors, increasing as the acidity does (PhOH < HFIP < PFTB). The IR and NMR data suggest C_{2v} symmetry around tungsten in the ROH···HW(CO)₂(NO)L₂ adduct, with the H···H distance of 1.77 Å (L = PMe₃) estimated from the hydride T_{1min} relaxation time. The relevance of the hydrogen bonding to the mechanism of protonation of metal hydrides is suggested.

Introduction

Hydrogen bonding is an important but generally weak (2–10 kcal/mol) chemical bonding phenomenon. It can occur both in intra- and intermolecular fashion between proton donor groups from one side and lone pairs of heteroatoms, π -electrons of aromatic rings, and multiple bonds from another.

More familiar as exemplified by organic molecules, hydrogen bonding has frequently been observed in transition metal complexes, and many structural components of organometallic or inorganic compounds are potential binding sites. In terms of a “natural” classification, known cases include hydrogen bonding to the metal centers and coordinated ligands and between the ligands.

The inter- and intramolecular interactions between N–H moieties and halide ligands or counterions (e.g., in complex **A**) have been thoroughly studied.¹ Other examples concern H-bonding to the oxygen atom of carbonyl and nitrosyl groups² as well as to π -ligands.^{2,3} Rather strong bonding of alcohols and phenols with alkoxy⁴ and phenoxy⁵ ligands has been established both in the solid state and in solution.

In a recent meticulous IR study,^{6a,b} hydrogen bonding of fluoro alcohols to the metal center of (η^5 -C₅H₅)ML₂ was clearly identified in liquid xenon and krypton. This novel type of bonding is also found and extensively studied for phenol and fluoro alcohols in regular nonpolar and low-polarity solvents.^{6c–e} Important examples of linear three-center four-electron H-bonds of the NH···M type are structurally characterized in the solid state;⁷ some of these also exhibit hydrogen bonding to the chlorine^{7a} and nitrogen^{7b} atoms of the counterions. Other investigations in organometallic solids show that complexes containing a hydrogen donor and accepting sites as COOH, OH, CH, COOR, and CO have features similar to those of related organic solids.⁸

Closely related to the matter of the present study are well-documented *intramolecular* interactions found between ligands with acidic hydrogen (NH, OH) and ligands representing weak

(4) (a) Kogley, S. E.; Schaverien, C.; Fredenberger, J. H.; Bergman, R. G.; Nolan, S. P.; Hoff, C. D. *J. Am. Chem. Soc.* **1987**, *109*, 6563. (b) Kim, Y. J.; Osakado, K.; Takenak, A.; Yamamoto, A. *J. Am. Chem. Soc.* **1990**, *112*, 1096.

(5) (a) Osakado, K.; Ohchiro, K.; Yamamoto, A. *Organometallics* **1991**, *10*, 404. (b) Alsters, P. L.; Baesjou, P. J.; Janssen, M. D.; Kooijman, H.; Sicherer-Roetman, A.; Spek, A. L.; Koten, G. *Organometallics* **1992**, *11*, 4124.

(6) (a) Kazarian, S. G.; Hamley, P. A.; Poliakov, M. *J. Chem. Soc., Chem. Commun.* **1992**, 994. (b) Kazarian, S. G.; Hamley, P. A.; Poliakov, M. *J. Am. Chem. Soc.* **1993**, *115*, 9069. (c) Vinogradova, L. E.; Kreindlin, A. Z.; Leytes, L. A.; Chizhevskii, I. T.; Shubina, E. S.; Epstein, L. M. *Organomet. Chem. USSR* **1990**, *3*, 618. (d) Epstein, L. M.; Shubina, E. S. *Metalloorg. Khim.* **1992**, *5*, 61. (e) Shubina, E. S.; Krylov, A. N.; Kreindlin, A. Z.; Rybinskaya, M. I.; Epstein, L. M. *THEOCHEM* **1993**, *301*, 1. (f) Epstein, L. M.; Krylov, A. N.; Shubina, E. S. *THEOCHEM* **1994**, *322*, 345.

(7) (a) Brammer, L.; Charnock, P. L.; Goggin, P. L.; Goodfellow, R. J.; Orpen, A. G.; Koetzle, T. F. *J. Chem. Soc., Dalton Trans.* **1991**, 1789. (b) Brammer, L.; McCann, M. C.; Bullock, R. M.; McMullen, R. K.; Sherwood, P. *Organometallics* **1992**, *11*, 2339. (c) Brammer, L.; Zhao, D. *Organometallics* **1994**, *13*, 1545.

(8) (a) Braga, D.; Grepioni, F.; Sabatino, P.; Desiraju, G. R. *Organometallics* **1994**, *13*, 3532. (b) Braga, D.; Grepioni, F.; Biradha, K.; Pedireddi, V. R.; Desiraju, G. R. *J. Am. Chem. Soc.* **1995**, *117*, 3156.

[†] Russian Academy of Sciences. Contributors of the IR work.

[‡] Universität Zürich. Contributors of the NMR work.

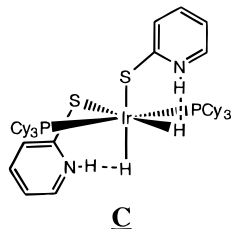
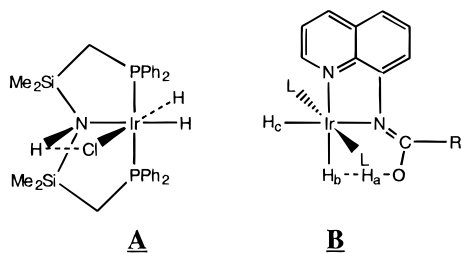
[⊗] Abstract published in *Advance ACS Abstracts*, January 15, 1996.

(1) (a) Fujita, J.; Kobayashi, M.; Nakamoto, K. *J. Am. Chem. Soc.* **1956**, *78*, 3295. (b) Osborn, J. A.; Powell, A. R.; Thomas, K.; Wilkinson, G. *J. Chem. Soc. A* **1968**, 1801. (c) Chatt, J.; Leigh, G. J.; Thankarajan, N. *J. Chem. Soc. A* **1971**, 3168. (d) Bronty, C.; Spinat, P.; Whuler, A. *Acta Crystallogr., Sect. B* **1980**, *36*, 1967. (e) Fryzuk, M. D.; MacNeil, P. A.; Rettig, S. J. *J. Am. Chem. Soc.* **1987**, *109*, 2803.

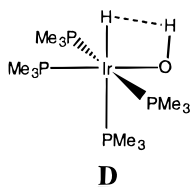
(2) (a) Lokshin, B. V.; Kazarian, S. G.; Ginzburg, A. G. *Izv. Akad. Nauk SSSR, Ser. Khim.* **1986**, 2605. (b) Lokshin, B. V.; Kazarian, S. G.; Ginzburg, A. G. *J. Mol. Struct.* **1988**, *174*, 29. (c) Lokshin, B. V.; Kazarian, S. G.; Ginzburg, A. G. *Izv. Akad. Nauk SSSR, Ser. Khim.* **1987**, 948. (d) Hamley, P. A.; Kazarian, S. G.; Poliakov, M. *Organometallics* **1994**, *13*, 1767.

(3) (a) Epstein, L. M.; Ashkinadze, L. D.; Rabiheva, S. O.; Kazitsyna, L. A. *Dokl. Akad. Nauk SSSR* **1970**, *190*, 128. (b) Cherichelli, G.; Illuminati, G.; Ortaggi, G.; Guilianto A. M. *J. Organomet. Chem.* **1977**, *127*, 357. (c) Alexanyan, V. G.; Kimel'fel'd, Ya. M.; Materikova, R. B.; Smirnova, G. M. *Zh. Fiz. Khim.* **1980**, *54*, 663.

bases such as halides and hydrides.⁹ Examples **B** and **C**, and, already mentioned above, **A** bear clear chemical resemblance, although there is a substantial difference in the nature of the bonding, which occurs with a lone pair of Cl in one case^{1c} and with the σ -bonding pair of Ir–H in the others.^{9c,d}



One (and chronologically the first) example of intramolecular M–H \cdots HO interaction was characterized by neutron diffraction, a method most reliable for location of hydrogens. In structure **D**, the H \cdots H distance is 2.40(1), which was interpreted as “too long for the interaction to be considered a normal hydrogen bond”.^{9c}



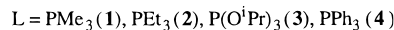
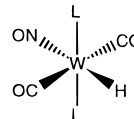
Complexes **B** and **C** and related molecules studied spectroscopically by NMR and IR (in few cases by X-ray) have intramolecular XH \cdots HM bonds of medium strength (estimated experimentally^{9d,f} and calculated^{9f} *ab initio* to be in the range 2.9–5 and 5–7 kcal/mol, respectively) with the H \cdots H distances of 1.7–1.8 Å.⁹

In this work, we experimentally address the problem of *intermolecular* XH \cdots HM hydrogen bonding in solution. Some fundamental differences between the *inter-* and *intramolecular* interactions should now be emphasized.

In the *intramolecular* case: (a) preassembling interacting fragments (ligands) at the metal center is, in a way, the driving force that might be responsible for the resulting geometry without any additional specific interligand interaction. More importantly, (b) for the thermodynamics of the system, intramolecular interaction does not necessarily require an entropy change, while an associative bimolecular process should assume $-\Delta S^\circ$ in the range of 5–20 eu.¹⁰ Then, at room temperature, $T\Delta S^\circ \leq 6$ kcal/mol, which represents a significant force against

bonding. Another important factor (c) is sterics: it should be difficult for a proton donor to get access to a binding site in a sterically crowded complex with bulky ligands (e.g., phosphines). Finally, (d) we do not know exactly how weak solvent–solute interaction can contribute to distinguish between the intra- and intermolecular cases. One should expect a greater influence for a bimolecular process.

For the present work, a series of tungsten monohydrides, known to have polarized metal–hydride bonds,¹¹ has been



selected and systematically studied in solution in the presence of acidic alcohols (phenol, hexafluoro-2-propanol (HFIP), and perfluoro-2-methyl-2-propanol (PFTB)). Here, we report the first IR and NMR spectroscopic evidence for the hydride of WH(CO)₂(NO)L₂ complexes acting indeed as a proton acceptor in *intermolecular* W–H \cdots H–O bonding. This evidence includes distinct changes of all significant IR bands (OH, CO, NO, and MH) as well as the following NMR parameters: shifts, couplings, and *T*₁ relaxation times. It becomes apparent that attractive X–H \cdots H–M interaction is a real driving force responsible for the specificity of protonation of hydride complexes, which as a rule occurs kinetically determined at the hydride site.¹²

Experimental Section

The monohydrides WH(CO)₂(NO)L₂ studied in this work were prepared as described elsewhere.^{11a} HFIP was purchased from Aldrich. (CF₃)₃COH was prepared as described in the literature.¹³

The IR spectra were recorded on a Specord M-82 spectrometer. All measurements were made under dry Ar atmosphere in freshly distilled oxygen-free nonpolar (hexane) and low-polarity media (hexane/CH₂Cl₂ 2:1). For the low-temperature experiments: cold (–100 °C) solutions of ROH and WH(CO)₂(NO)L₂ were mixed and transferred into the precooled cell (*d* = 0.1 cm) of the cryostat against counterflow of argon. These experiments were run from 190 to 250 K. The error of the temperature determination was ± 0.5 K.

For the NMR samples, in a typical case: HFIP solution in dry, oxygen-free solvent (CD₂Cl₂, toluene-*d*₆) (0.65 mL) was prepared under nitrogen in a dry box in a Schlenk flask fitted with Teflon stopcock. This solution was vacuum transferred into a 5 mm NMR tube containing a weighed amount of WH(CO)₂(NO)L₂ and the tube was then flame sealed under vacuum and transferred into a cold (–100 °C) ethanol bath. The NMR experiments were run starting at low temperatures on a Varian Gemini 300 spectrometer. Standard Varian software was used for the inversion-recovery *T*₁ determinations and NOE (DIFNOE) measurements.

Results and Discussion

I. IR Evidence for Hydrogen Bonding of Phenols and Fluoro Alcohols with WH(CO)₂(NO)L₂ (L = PMe₃ (**1**), PEt₃ (**2**), P(OⁱPr)₃ (**3**), and PPh₃ (**4**)). (a) ν (OH) Range. The first

(10) (a) Jaffe, H. H. *J. Am. Chem. Soc.* **1957**, *79*, 2373. (b) Arnett, E. M.; Joris, L.; Mitchell, E.; Murty, T. S. S. R.; Gorrie, T. M.; Schleyer, P. v. R. *J. Am. Chem. Soc.* **1970**, *92*, 2365. (c) Lopes, M. C. S.; Thompson, H. W. *Spectrochim. Acta* **1968**, *24A*, 1367.

(11) (a) van der Zeijden, A. A. H.; Sontag, C.; Bosch, W.; Shklover, V.; Berke, H.; Nanz, D.; von Philipsborn, W. *Helvetica Chim. Acta* **1991**, *74*, 1194. (b) van der Zeijden, A. A. H.; Bürgi, T.; Berke, H. *Inorg. Chem.* **1992**, *201*, 131. (c) Berke, H.; Burger, P. *Comments Inorg. Chem.* **1994**, *16*, 279.

(12) (a) Jessop, P. G.; Morris, H. *Coord. Chem. Rev.* **1992**, *121*, 155. (b) Heinekey, D. M.; Oldham, W. J., Jr. *Chem. Rev.* **1993**, *93*, 913.

(13) Filler, R.; Schure, R. M. *J. Org. Chem.* **1967**, *32*, 1217.

(14) Cabana, A.; Sandorfy, C. *Spectrochim. Acta* **1960**, *16*, 335.

(9) (a) Lough, A. J.; Park, S.; Ramachandran, R.; Morris, R. H. *J. Am. Chem. Soc.* **1994**, *116*, 8356. (b) Park, S.; Ramachandran, R.; Lough, A. J.; Morris, R. H. *J. Chem. Soc., Chem. Commun.* **1994**, 2201. (c) Lee, J. C.; Rheingold, A. L.; Muller, B.; Pregosin, P. S.; Crabtree, R. H. *J. Chem. Soc., Chem. Commun.* **1994**, 1021. (d) Lee, J. C.; Peris, E.; Rheingold, A. L.; Crabtree, R. H. *J. Am. Chem. Soc.* **1994**, *116*, 11014. (e) Stevens, R. C.; Bau, R.; Milstein, D.; Blum, O.; Koetzle, T. F. *J. Chem. Soc., Dalton Trans.* **1990**, 1429. (f) Peris, E.; Lee, J. C.; Rambo, J. R.; Eisenstein, O.; Crabtree, R. H. *J. Am. Chem. Soc.* **1995**, *117*, 3485.

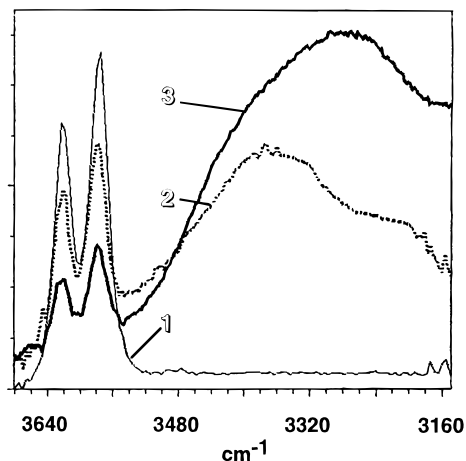


Figure 1. IR spectra in the $\nu(\text{OH})$ absorption region of (1) HFIP (0.01 mol/L), (2) HFIP/WH(CO)₂(NO)[P(O^{*t*}Pr)₃]₂ (0.01/0.05 mol/L), and (3) HFIP/WH(CO)₂(NO)(PMe₃)₂ (0.01/0.05 mol/L).

Table 1. $\nu(\text{OH})$ Absorptions (cm⁻¹) of PhOH, HFIP, and PFTB in the Presence of WH(CO)₂(NO)L₂ 1–4 in Hexane

L	proton donor	$\nu(\text{OH})_{\text{bonded}}^a$	$\Delta\nu_{1/2}$	$\Delta\nu(\text{OH})^b$	$A(\text{OH})_{\text{bonded}}^c$ 10 ⁻⁴ L/mol·cm ²
PMe ₃ (1)	PhOH	3328	180	295	8.3
	HFIP	3288	235	323	9.1
	PFTB	3140	390	448	12.9
PEt ₃ (2)	PhOH	3350	190	273	7.6
	HFIP	3308	314	302	8.1
	PFTB	3183	384	405	11.7
P(O ^{<i>i</i>} Pr) ₃ (3)	HFIP	3375	176	236	6.4
	PFTB	3262	233	320	9.4
PPh ₃ ^d (4)	HFIP	3375	150	215	<i>e</i>

^a Values correspond to the centers of gravity of the $\nu(\text{OH})_{\text{bonded}}$ bands.

^b $\nu(\text{OH})_{\text{free}} = 3623$ (PhOH), 3631 and 3592 (HFIP), 3588 cm⁻¹ (PFTB). For HFIP, $\Delta\nu(\text{OH})$ is calculated from the center of the double band.

^c Integral intensities $A(\text{OH})_{\text{bonded}}$ were calculated by the method of ref 14. ^d Data from solution in hexane/CH₂Cl₂ (2:1). ^e Accurate determination was impossible because the solubility was too low.

spectroscopic evidence for hydrogen bonding is often provided by IR investigations in the absorption region of X–H vibrations of the proton donors. When there is hydrogen bonding of XH functionalities, broad $\nu(\text{XH})$ bands are expected to appear, shifted to lower frequencies and increased in intensity.

The IR spectra of HFIP, PFTB, and phenol (concentrations of ROH varied in the range 0.005–0.01 mol/L to exclude self-association) were measured in hexane in the presence of an excess of complexes 1–3. A hexane/methylene chloride (2:1) mixture was used for complex 4, which is insoluble in hexane.

Interaction between the alcohols and hydrides 1–4 brings about the appearance of broad and intense IR bands over the range 3100–3400 cm⁻¹ (Figure 1). These spectral changes are indeed diagnostic for hydrogen bonding, and new bands are assigned to $\nu(\text{OH})_{\text{bonded}}$ vibrations. Data in Table 1 show how the shift ($\Delta\nu(\text{OH})$), width ($\Delta\nu_{1/2}$), and integral intensity ($A(\text{OH})$) of the $\nu(\text{OH})_{\text{bonded}}$ bands depend on electronic properties of the phosphorus ligands in 1–4. The effect of changing phosphine donicity is clear: $\nu(\text{OH})$ shifts to lower wavenumbers and the value of $\Delta\nu_{1/2}$ increases on going from L = P(O^{*i*}Pr)₃ (3) to more basic PEt₃ in 2 and (also less bulky) PMe₃ in 1 for each proton donor used. The spectral parameters depend on the acidity of the alcohols as well, and the shift $\Delta\nu(\text{OH})$ increases when the acidity does, for instance, for 2: $\nu(\text{OH})_{\text{bonded}} = 3328$ (PhOH, $pK_a = 10.0$) > 3267 (HFIP, $pK_a = 9.2$) > 3150 cm⁻¹ (PFTB, $pK_a = 5.4$).

The IR data in the $\nu(\text{OH})$ range represent certain spectroscopic evidence for hydrogen bonding between WH(CO)₂(NO)L₂ and

Table 2. $\nu(\text{CO})$ Bands (cm⁻¹) of the Complexes 1–4 with HFIP at 200 K in Hexane

L	$\nu(\text{CO})_{\text{free}}$	$\nu(\text{CO})_{\text{bonded}}$	$\Delta\nu(\text{CO})$
PMe ₃ (1)	1914	1924	10
PEt ₃ (2)	1908	1922	14
P(O ^{<i>i</i>} Pr) ₃ (3)	1929	1944	13
PPh ₃ ^a (4)	1930	1945	15

^a In a mixture hexane/CH₂Cl₂ (2:1).

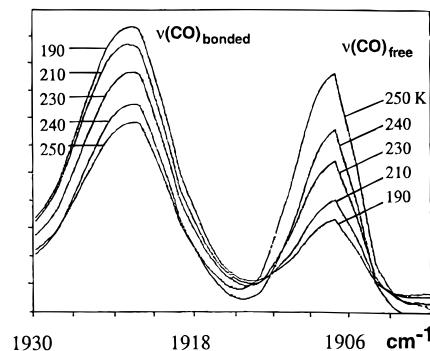


Figure 2. Variable-temperature IR spectra of WH(CO)₂(NO)(PEt₃)₂/HFIP (0.001/0.008 mol/L) in hexane in the range 1900–1930 cm⁻¹.

the alcohols, but they provide no structural information. In particular, there is no clue to which of the four potential sites (H, CO, NO, W) is engaged in the bonding. We therefore thoroughly investigated the absorption region of the $\nu(\text{CO})$, $\nu(\text{NO})$, and $\nu(\text{WH})$ vibrations.

(b) $\nu(\text{CO})$, $\nu(\text{NO})$, and $\nu(\text{WH})$ IR Data. The IR spectra of solutions containing WH(CO)₂(NO)L₂ and an excess of the proton donors reveal the appearance of *one new* $\nu(\text{CO})$ band, shifted by $\Delta\nu(\text{CO}) = 10$ –17 cm⁻¹ to *higher* wavenumbers with reference to the corresponding $\nu(\text{CO})_{\text{free}}$ vibration in 1–4 (Table 2). The intensity of this new band is temperature dependent and increases (by decrease of the intensity of $\nu(\text{CO})_{\text{free}}$) on lowering the temperature (Figure 2). These intensity changes are reversible, indicating that formation of the new species is an equilibrium process.

The shift $\Delta\nu(\text{CO})$ shows dependence on the proton-donating ability (acidity) of the alcohols and increases when the latter does. For example, for complex 2 $\Delta\nu(\text{CO}) = 11$ (PhOH) < 14 (HFIP) < 17 cm⁻¹ (PFTB). The magnitude of $\Delta\nu(\text{CO})$ independently suggests assignment of the shifted band to some hydrogen-bonded species; a much greater shift, 100–150 cm⁻¹, would have been observed if the metal center had been protonated.^{6b,f} Another conclusive piece of information is worth mentioning: hydrogen bonding to the oxygen atom of CO in a O–H···O–C–M fashion, if it were present, would cause shifts to *lower* wavenumbers of at least one $\nu(\text{CO})$ vibration,^{2a,b} i.e., the opposite to what is observed in 1–4.

Some significant structural conclusions are now rendered possible. The observation of a single $\nu(\text{CO})_{\text{bonded}}$ band for the H-bonded species ROH&WH(CO)₂(NO)L₂ suggests that the local symmetry around the metal center is retained. This implies that ROH approaches the complex in the plane perpendicular to the OC–W–CO axis. The bonding site is, thus, either the nitrosyl or the hydride ligand of WH(CO)₂(NO)L₂. We will show further how the ¹H NMR data most reliably establish that it is the hydride location that is attacked. This conclusion is well supported by the IR data, which show *high-wavenumber* and *low-wavenumber* shoulders in the $\nu(\text{NO})$ and $\nu(\text{WH})$ bands, respectively, in the presence of ROH (Figure 3a). The former feature is better resolved (Figure 3b) in the WD(CO)₂(NO)-(PEt₃)₂-HFIP system, where the W–D and N–O vibrations are not coupled.^{11a} The trend shown by the WH and NO bands

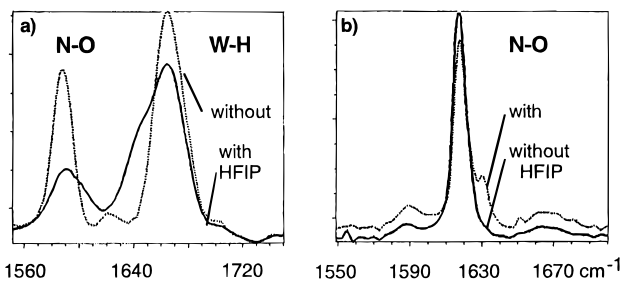


Figure 3. IR spectra of (a) $\text{WH}(\text{CO})_2(\text{NO})(\text{PEt}_3)_2/\text{HFIP}$ (0.004/0.012 mol/L) and (b) $\text{WD}(\text{CO})_2(\text{NO})(\text{PEt}_3)_2/\text{HFIP}$ (0.004/0.012 mol/L) at 200 K in hexane. In b, weak bands at 1589 and 1670 cm^{-1} are due to remaining $\text{WH}(\text{CO})_2(\text{NO})(\text{PEt}_3)_2$.

clearly speaks against ROH binding to the nitrosyl oxygen (a shift to low frequencies would then be expected^{2c}), neither does it support $\text{OH}\cdots\text{W}$ hydrogen bonding (a shift to higher frequencies is expected for $\nu(\text{WH})$ when the electron density on the metal is decreased¹⁵).

The possibility of some interaction between the oxygen atom of the alcohols and the metal itself was also taken into consideration (this would have occurred in the vicinity of the hydride ligand in any case). It is doubtful that the oxygen atom can coordinate to an 18e metal center; the IR spectra of $\text{WH}(\text{CO})_2(\text{NO})(\text{PEt}_3)_2$ show unchanged $\nu(\text{CO})$, $\nu(\text{NO})$, and $\nu(\text{WH})$ bands in the presence of other oxygen donors like Pr_2O and PhOCH_3 .

(c) Strength of the $\text{OH}\cdots\text{HW}$ Hydrogen Bond. Changes in the $\nu(\text{OH})$ region, described above, reflect the strength of hydrogen bonding: both the band shifts $\Delta\nu(\text{OH})$ and the integral intensities $A(\text{OH})_{\text{bonded}}$ correlate with the enthalpy of the bonding, $-\Delta H^\circ$. Different equations have been suggested to quantify this.¹⁶ We applied here those proposed by Iogansen (initially for organic molecules): eqs 1 and 2 have been successfully used to characterize hydrogen bonding in a number of precedents in organometallic systems.^{6a,b,d-f} Correlation eq

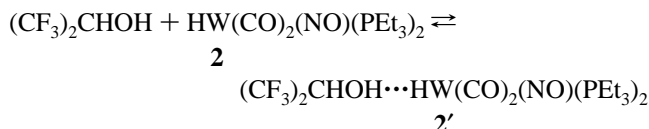
$$-\Delta H^\circ = 18\Delta\nu(\text{OH})/(\Delta\nu(\text{OH}) + 720) \quad (1)$$

$$-\Delta H^\circ = 0.30(\Delta\nu(\text{OH}))^{1/2} \quad (2)$$

$$-\Delta H^\circ = 2.9(\Delta A(\text{OH}))^{1/2} \quad (3)$$

1 is considered to be more general and applicable in the range of $\Delta\nu(\text{OH}) = 0\text{--}2000 \text{ cm}^{-1}$, while eq 2 is limited to the cases when $\Delta\nu(\text{OH}) > 200 \text{ cm}^{-1}$. Most versatile is eq 3¹⁷, which we use here for the first time as applied to H-bonding with a metal complex. Table 3 shows that all correlations provide consistent results.

Experimental values of $K = [2']/([2][\text{HFIP}])$ were determined for the equilibrium



by measuring the absorption of $\nu(\text{CO})_{\text{free}}$ band over the

(15) Girling, R. B.; Grebenik, P.; Perutz, R. N. *Inorg. Chem.* **1986**, *25*, 31.

(16) (a) Badger, R. M.; Bauer, S. H. *J. Chem. Phys.* **1937**, *5*, 839. (b) Iogansen, A. V.; Kurkchi, G. A.; Furman, V. M.; Glazunov, V. P.; Odionov, S. E. *Zh. Prikl. Spektrosk.* **1980**, *33*, 460. (c) Iogansen, A. V. *Hydrogen Bond*; Nauka: Moscow, 1981; p. 13. (d) Zeegers-Huyskens, T. In *Intermolecular Forces; An Introduction to Modern Methods and Results*; Huyskens, P. L., Luck, W. A. P., Zeegers-Huyskens, T., Eds.; Springer-Verlag: Berlin, 1991; p. 123.

(17) $\Delta A(\text{OH})^{1/2} = A(\text{OH})_{\text{free}}^{1/2} - A(\text{OH})_{\text{bonded}}^{1/2}$.

Table 3. Enthalpies of Hydrogen Bond Formation $-\Delta H^\circ$ (kcal/mol) and Basicity Factors Calculated from eqs 1–4

L	proton donor	$-\Delta H^\circ(1)$	$-\Delta H^\circ(2)$	$-\Delta H^\circ(3)$	E_j^a
PMe ₃ (1)	PhOH	5.2	5.2	5.2	0.92
	HFIP	5.6	5.5	5.6	0.91
	PFTB	6.9	6.5	6.8	0.90
PEt ₃ (2)	PhOH	5.0	5.1	4.9	0.87
	HFIP	5.3	5.3	5.1	0.87
	PFTB	6.5	6.2	6.4	0.85
P(O ⁱ Pr) ₃ (3)	HFIP	4.4	4.7	4.2	0.73
	PFTB	5.5	5.5	5.3	0.72
PPh ₃ (4)	HFIP	4.1	4.5	<i>b</i>	0.70

^a Basicity factors calculated from eq 4 using $\Delta H^\circ(1\text{--}3)$ and averaged to give E_j reported in this table. ^b Integral intensity is not available in this case (see also Table 1).

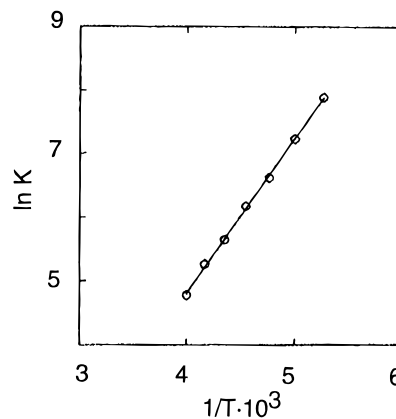


Figure 4. $\ln K$ vs. $1/T$ for $\text{WH}(\text{CO})_2(\text{NO})(\text{PEt}_3)_2/\text{HFIP}$ (0.001/0.004 mol/L) in the range 190–250 K.

temperature range 190–250 K.¹⁸ The temperature dependence $\ln K$ vs $1/T$, presented in Figure 4, gives $-\Delta H^\circ = 4.9 \pm 0.3$ kcal/mol, in agreement with the values (5.1–5.3 kcal/mol) calculated in Table 3. The value of $\Delta S^\circ = -9.8 \pm 1$ eu, determined from the plot in Figure 4, lies in the range (5–20 eu) reported for hydrogen bonding in organic systems.^{10bc,19} Similar characteristics are, for example, known for *p*-fluorophenol with *N*-methylformamide ($-\Delta H^\circ = 5.5$ kcal/mol, $\Delta S^\circ = -9.5$ eu).^{10b}

Hydrogen bonding of the alcohols to the hydrides **1–4** is of medium strength (4.1–6.9 kcal/mol), comparable to that determined for the bonding of $\text{M}\cdots\text{HOR}$.⁶ These values are also close to the estimated energy of *intramolecular* Ir–H \cdots H–N hydrogen bonds (3–5 kcal/mol).^{9d,f} For all $\text{WH}(\text{CO})_2(\text{NO})\text{L}_2$ derivatives the association enthalpy $-\Delta H^\circ$ parallels the proton donating ability (acidity) of the alcohols. For complex **2**, for instance, it increases in the order 4.9 (PhOH) < 5.1 (HFIP) < 6.4 kcal/mol (PFTB).

Another empirical correlation seems to be perfectly applicable in our system. Introduced by Iogansen, the “factor of basicity”, E_j , is expected to characterize the proton accepting site in hydrogen bond formation.²⁰

$$E_j = \Delta H_{ij}/5.7P_i \quad (4)$$

where P_i is the acidity factor for the proton donor and $\Delta H_{ij} = -\Delta H^\circ$.^{20b}

E_j for **1–4** must show no dependence on the acidity of the proton donors, and they are constant indeed: for example, 0.91

(18) Equilibrium concentrations were calculated from the decrease of $\nu(\text{CO})_{\text{free}}$ band intensity for every temperature.

(19) In the case of hydrogen bonding to the metal, HFIP–Cp*Ir(CO)₂, a larger change $\Delta S = -19$ eu is reported.^{6a}

± 0.01 for **1** with all ROH in this work (Table 3). There is, however, expected dependence of the calculated proton accepting ability E_j of the hydridic hydrogen in **1–4** on the electronic and steric properties of the phosphines:²¹ cone angle/basicity = 145/2.73 PPh₃, 130/4.08 P(OⁱPr)₃, 132/8.69 PEt₃, 118/8.65 PMe₃. Values of E_j increase in the same order: PPh₃ < P(OⁱPr)₃ < PEt₃ < PMe₃ (Table 3). The E_j 's for **1** and **2** are rather close (0.91 vs. 0.87) but lower for **3** and **4** (0.72 and 0.70, respectively).

II. NMR Evidence for the Interaction between the WH(CO)₂(NO)L₂ Complexes 1–4 and HFIP. The IR data give clear evidence for hydrogen bonding between the WH(CO)₂(NO)L₂ complexes **1–4** and HFIP. In this section, we attempt characterization of this interaction by NMR, a relatively "slow" spectroscopic method. The energies estimated above (4–7 kcal/mol) suggest that association and dissociation of the molecules (exchange) must be fast on the NMR time scale. This should result in averaging of all NMR parameters in the available temperature range.

Another circumstance, which unfavorably distinguishes NMR from IR, is the natural demand of the method for higher concentrations and the use of deuterated solvents. In the solvents employed here, CD₂Cl₂ and toluene-*d*₈, the complexes show different stability: as all stable are in toluene (within the time of the measurements), there were two representatives (L = PMe₃ and PEt₃) subjected to protonation by HFIP in CD₂Cl₂. In this solvent, WH(CO)₂(NO)(PMe₃)₂ is especially unstable even at low temperature, and therefore no reliable data could be collected.

(a) Temperature and Concentration Dependence of the W–H Chemical Shift. IR spectroscopically we have observed the tightest adduct formation for HFIP with WH(CO)₂(NO)(PMe₃)₂ (**1**). This complex was selected for a series of NMR experiments in toluene-*d*₈ with concentration of HFIP varying from nil to 0.19 mol/L and the tungsten concentration [**1**] constant at 0.06 mol/L, i.e., the ratio of both species increased from 0 to 3.2.

The ¹H NMR spectra of these solutions, recorded between –70 and –100 °C, show resonances of the CH₃, CH, WH, and OH protons, with remarkable changes revealed by the latter two. The OH proton appears as a broad (40–100 Hz) line that shifts from δ 4 to 7 ppm progressively upon cooling and/or decreasing the concentration of HFIP in solution. The hydride triplet of WH(CO)₂(NO)(PMe₃)₂ broadens by 2–4 Hz upon lowering the temperature and/or increase of the HFIP concentration. The line width reaches the maximum of 7 Hz at –100 °C; a sample without HFIP is 3 Hz broad at this temperature. The direction of the change of the chemical shift δ (WH) is less apparent than that for OH: the hydride resonance drifts upfield. In the most concentrated sample the resulting shift (from δ (WH) –1.41 in **1**) is remarkably large: $\Delta\delta$ is 0.72 ppm at –100 °C.

(20) (a) Iogansen, A. V. *Theor. Exp. Khim.* **1971**, 7, 302. (b) As a result of analysis of a large array of spectroscopic and calorimetric data (in particular for phenols and fluorinated alcohols) Iogansen introduced what he named a "rule of factors", an empirical correlation assuming constant acidic and basic properties in hydrogen bond formation. The general equation for a proton donor *i* and acceptor *j* is: $\Delta X_{ij} = \Delta X_i P_i E_j$, where ΔX stands for either a spectroscopic ($\Delta\nu$, ΔA) or thermodynamic ($-\Delta H^\circ$) characteristic in a specific solvent; that on the right side is for the "standard" H-bonded complex, phenol–ether ($-\Delta H^\circ_s = 5.7$ kcal/mol). For the standard complex both the basicity and acidity factors then are taken as unity, $E_j = P_i = 1$. The acidity factors of the other alcohols in this work are 1.07 (HFIP) and 1.31 (PTFB), which permits calculation of E_j for any of the partners in hydrogen bonding, complexes **1–4**.

(21) (a) Tolman, C. A. *Chem. Rev.* **1977**, 77, 313. (b) Rahman, M. M.; Liu, H.-Y.; Eriks, K.; Prock, A.; Giering, W. P. *Organometallics* **1989**, 8, 1.

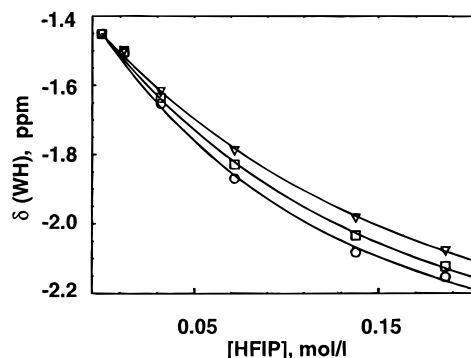
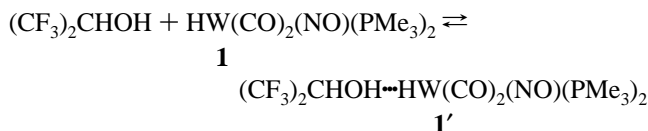


Figure 5. Hydride chemical shift δ (WH) in WH(CO)₂(NO)(PMe₃)₂ (0.06 mol/L) at –70 (▽), –80 (◻), –90 °C (○) in toluene-*d*₈ solutions containing variable amounts of HFIP.

Figure 5 shows the concentration dependence of δ (WH) at three temperatures (from –70 to –90 °C). Assuming a fast bimolecular reaction,



one can relate the averaged chemical shift δ (WH) to the chemical shifts of the free and hydrogen bonded complexes, δ_1 and δ_2 , via the equilibrium constant (*K*) and the initial concentrations of WH(CO)₂(NO)L₂ (*w*) and HFIP, the latter being expressed as *x*.

$$\delta(\text{WH}) = (\delta_1 + 0.5\delta_2((a^2 + 4Kx)^{1/2} - a)) / (1 + 0.5((a^2 + 4Kx)^{1/2} - a))$$

where $a = Kw - Kx + 1$.

By computer fitting of the experimental data to the above equation, the two unknown parameters, *K* and δ_2 , were determined. The chemical shift in the hydrogen-bonded complex **1'**, δ_2 , expectedly shows no significant variation between –70 and –90 °C as -2.67 ± 0.05 ppm. The equilibrium constant increases from 6.3 (–70 °C) to 10.8 L/mol (–90 °C). The magnitude of *K* implies some small free energy change ΔG of ca. –0.7 kcal/mol in favor of the hydrogen bonded complex formation; this gives a qualitative picture for the thermodynamics of the bonding under conditions of the NMR experiments.

The experimental (IR) values of *K* in *hexane* are between 140 (–23 °C) and 3000 L/mol (–83 °C) for the system HFIP/complex **2** (Figure 4). It appears, therefore, that equilibrium constants for the HFIP binding to **1** in *hexane* must also be appreciably higher than those in *toluene*, derived from the NMR analysis. We have no clear understanding for this observation. Two possible reasons can be mentioned. One is that the thermodynamics in the NMR experiments is influenced by the higher concentration and, thus, self-association of the HFIP molecules. The second explanation assumes that the thermodynamics can be affected by hydrogen bonding of HFIP to the aromatic ring of the solvent, toluene-*d*₈.

(b) T₁(WH) Relaxation Time. Spin-lattice relaxation of the hydride ligand in all WH(CO)₂(NO)L₂ is clearly dominated by proton–proton dipole–dipole interactions. The strength of the interaction is strongly distance dependent: *T*₁ is proportional to $r^{-6}(\text{H}\cdots\text{H})$. These factors make *T*₁ measurements probably the most reliable and sensitive experiment to determine ROH...

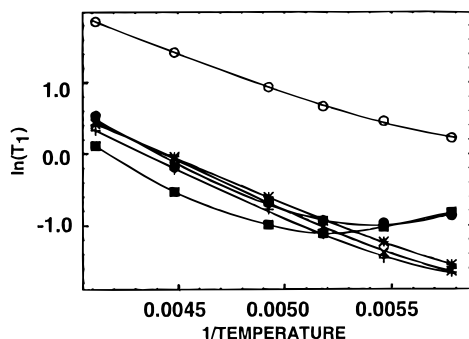


Figure 6. Variable-temperature ^1H T_1 relaxation times in $\text{WH}(\text{CO})_2(\text{NO})(\text{PMe}_3)_2/\text{HFIP}$. $T_1(\text{WH})$: \circ , \bullet , \blacksquare . $T_1(\text{CH}_3)$: $*$, \times , $+$. The concentrations are 0.034/0, 0.034/0.125, and 0.056/0.186 mol/L, respectively.

$\text{HW}(\text{CO})_2(\text{NO})\text{L}_2$ bonding: if OH in **1'** is close to WH, there must be substantially faster relaxation (shorter T_1) of the metal-bound proton.

Figure 6 shows the ^1H T_1 relaxation times in $\text{WH}(\text{CO})_2(\text{NO})(\text{PMe}_3)_2$ in the presence/absence of HFIP. A small difference is expected and observed for the methyl protons; after addition of HFIP the relaxation times are close to those measured for **1** alone. The hydride T_1 changes abruptly: there is a 3-fold decrease from the estimated $T_{1\text{min}}$ of 1.15 s in $\text{WH}(\text{CO})_2(\text{NO})(\text{PMe}_3)_2$ without HFIP to 0.38 s when $[\text{1}]/[\text{HFIP}] = 0.034/0.125$ mol/L. Further shortening of $T_{1\text{min}}$ to 0.33 s is apparent in a more concentrated sample (0.056/0.186 mol/L), reflecting the equilibrium shift to form more **1'**.

For the simplest model assuming bonding of one molecule of HFIP to $\text{WH}(\text{CO})_2(\text{NO})(\text{PMe}_3)_2$, the change in T_1 is due to the contribution (ΔR_1) from dipole-dipole interaction between the alcoholic proton and the metal hydride separated by some distance $r(\text{H}\cdots\text{H})$. This distance can be easily estimated from the following equation:²² $r(\text{H}\cdots\text{H})$ (\AA) = $5.817(\nu\Delta R_{1\text{min}})^{-1/6}$, where ν is the NMR frequency in MHz and $\Delta R_{1\text{min}}$ is a difference between $1/T_{1\text{min}}$ in **1'** and **1**.

In the present case, the equilibrium constant at the temperature when $T_{1\text{min}}$ is observed (-80 °C) is 8.0 L/mol. This estimates 47 and 55% of the hydrogen-bonded complex in fast equilibrium with free $\text{WH}(\text{CO})_2(\text{NO})(\text{PMe}_3)_2$ (tungsten/alcohol concentrations are 0.034/0.125 and 0.056/0.186 mol/L, respectively). This in turn permits the calculation of true $1/T_{1\text{min}} = 5.05 \text{ s}^{-1}$ in the hydrogen-bonded complex **1'** from the exchange-averaged $T_{1\text{min}}$ values of 0.38 and 0.33 s and T_1 of 1.94 s in **1** at -80 °C. Consequently, the relaxation contribution from the $\text{H}\cdots\text{H}$ bonding, $\Delta R_{1\text{min}}$, is 4.18 s^{-1} and $r(\text{H}\cdots\text{H}) = 1.77 \text{ \AA}$.

This distance is in the range of values (1.7–1.9 \AA) reported recently for the $\text{NH}\cdots\text{H}\text{Ir}$ and $\text{OH}\cdots\text{H}\text{Ir}$ intramolecular hydrogen bonds⁹ and represents clear evidence for assigning the hydride in **1'** as the proton accepting site.

(c) NOE Difference Data. From the T_1 relaxation data presented above, some NOE is anticipated between the OH and WH protons, which must be a case of "transferred NOE" or TRNOE.²³ In a series of experiments with $\text{WH}(\text{CO})_2(\text{NO})(\text{PMe}_3)_2/\text{HFIP}$ (0.056/0.186 mol/L) in toluene- d_8 this was in fact clearly detected.

At -30 °C, irradiation of the OH resonance leads to 11% enhancement of the WH triplet. On lowering the temperature this effect gets weaker and then changes the sign (for a detailed

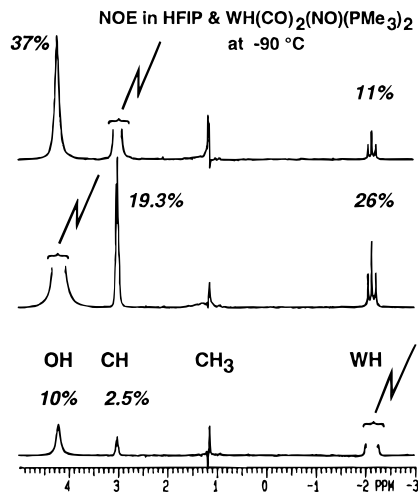


Figure 7. ^1H NOE difference spectra of $\text{WH}(\text{CO})_2(\text{NO})(\text{PMe}_3)_2/\text{HFIP}$ (0.056/0.186 mol/L) in toluene- d_8 at -90 °C. The irradiated positions are indicated with thunderbolt signs.

discussion of the temperature dependence of NOE see ref 24). At -90 °C, negative NOE is remarkably strong between the protons (OH, CH) of HFIP and WH (Figure 7): irradiation of OH gives 19.3 and 26% decreases of CH and WH, and irradiation of WH reduces the signal intensities of OH and CH by 10 and 2.5%, respectively. Finally, when the decoupler is applied at the frequency of CH, there are negative NOE's of 37% for OH and 11% for WH. Practically no NOE was detected in these experiments between the irradiated protons and the CH_3 groups of the PMe_3 ligands.

These NOE results provide unambiguous evidence for hydrogen bonding between HFIP and $\text{WH}(\text{CO})_2(\text{NO})(\text{PMe}_3)_2$ that brings the OH and WH protons together and establishes an additional (longer) contact between the hydride and CH of HFIP.

One circumstance in the relaxation and NOE data presented above deserves special comment. The observation of negative NOE indicates that the internuclear vector connecting OH and HW protons in **1'** has a slow tumbling rate on the NMR time scale at -90 °C, i.e., the correlation time $\tau_c < 1/\omega$ ($\omega = 2\pi\nu$). This is also supported by direct observation of the T_1 minimum in Figure 6 at about -80 °C, when $\tau_c = 0.62/\omega$. For complex **1** the minimum is predicted by fitting the data in Figure 5 at about -110 °C. Physical meaning of the observed shift of the $T_{1\text{min}}$ temperature is clear: hydrogen bonding of HFIP to $\text{WH}(\text{CO})_2(\text{NO})(\text{PMe}_3)_2$ increases the effective size of the tungsten complex which makes the tumbling slower and correlation time longer. Total motion of the aggregate is apparently anisotropic, since the methyl protons have $T_{1\text{min}}$ at some lower temperature. We have already observed distinct cases of this behavior for rhenium hydrides,^{25a} and related examples are known for macromolecules.^{25b}

(d) H–P Coupling Constant. The two-bond hydride–phosphorus coupling in $\text{WH}(\text{CO})_2(\text{NO})(\text{PMe}_3)_2$ shows no temperature dependence. Measured as a distance between the outermost transitions, i.e., being $2^2J(\text{H–P})$, it is 51.0–51.5 Hz between -30 and -100 °C. In the sample containing an excess of HFIP (0.125–0.034 mol/L), this coupling steadily decreased on lowering the temperature from 48.4 at -30 °C to 46.7 Hz at -100 °C. Gradual decrease of the coupling was also evident in experiments with an increasing $[\text{HFIP}]/[\text{1}]$ ratio: 51.0 (0.32:

(22) Desrosiers, L. H.; Cai, Z. R.; Lin, R.; Richards, R.; Halpern, J. J. *Am. Chem. Soc.* **1991**, *113*, 4173.

(23) Neuhaus, D.; Williamson, M. P. *The Nuclear Overhauser Effect in Structural and Conformational Analysis*; VCH Publishers, Inc.: New York, 1989; pp 175–181.

(24) Neuhaus, D.; Williamson, M. P. *The Nuclear Overhauser Effect in Structural and Conformational Analysis*; VCH Publishers, Inc.: New York, 1989; pp 89–94.

(25) (a) Gusev, D. G.; Nietispach, D.; Vymenits, A. B.; Bakhmutov, V. I.; Berke, H. *Inorg. Chem.* **1993**, *32*, 3270. (b) Ley, S. V.; Neuhaus, D.; Williams, D. J. *Tetrahedron Lett.* **1982**, *23*, 1207.

Table 4. ^1H NMR Data^a for the Hydride Resonances of $\text{WH}(\text{CO})_2(\text{NO})\text{L}_2$ without and with Added HFIP

L	solvent: [W]/[HFIP] ^b	δ (ppm) without/with	$^2J(\text{H}-\text{P})$ (Hz) without/with	$T_{1\text{min}}$ (ms) without/with	ΔR_1^c (s ⁻¹)
PMe_3 (1)	toluene- <i>d</i> ₈ 0.034/0.12	-1.45/-2.06 $\Delta\delta = 0.61$	51.5/47.0	1147/380	1.76
PEt_3 (2)	toluene- <i>d</i> ₈ 0.036/0.11	-1.96/-2.08 $\Delta\delta = 0.12$	46.1/45.8	764/455	0.89
	CD_2Cl_2 0.043/0.10	-2.61/-2.94 $\Delta\delta = 0.33$	46.6/44.3	718/349	1.47
$\text{P}(\text{O}^i\text{Pr})_3$ (3)	CD_2Cl_2 0.027/0.040	-2.19/-2.41 $\Delta\delta = 0.22$	63.4/62.2	700/460	0.75
PPh_3 (4)	CD_2Cl_2 0.023/0.034	-0.37/-0.40 $\Delta\delta = 0.03$	44.1/44.0	635/544	0.26

^a The chemical shifts and couplings at -90°C . ^b Concentrations: [complex]/[HFIP], mol/L. ^c Difference in the relaxation rates calculated as $1/T_{1\text{min}}(\text{with}) - 1/T_{1\text{min}}(\text{without HFIP})$.

1), 50.2 (0.54:1), 48.3 (1.2:1), 47.0 Hz (2.3:1). These data were taken at -90°C , at a constant concentration of **1** (0.06 mol/L).

In none of the experiments did we note any appreciable variation of the hydride coupling to the metal, ^{183}W nucleus. This certainly correlates with the IR observation of only subtle changes in the W—H stretching frequency upon addition of HFIP. The energy of the hydrogen bonding, 4–5 kcal/mol, is 1 order of magnitude weaker than the energy of typical metal–hydride bonds (50–75 kcal/mol) and can, in fact, only slightly perturb the hydride binding to tungsten. Any changes of $^2J(\text{H}-\text{P})$ must be attributed to some conformational deformations in the complex. This coupling is a sensitive function of the H—M—P angle, and even slight bending of the phosphorus ligands (caused by addition of HFIP) might change it by some Hz.²⁶

(e) How Does the Interaction between HFIP and $\text{WH}(\text{CO})_2(\text{NO})\text{L}_2$ Depend on the Nature of L? In this section we will show how addition of HFIP results in distinct changes of $\delta(\text{WH})$, $^2J(\text{H}-\text{P})$, and $T_1(\text{WH})$ in the $\text{WH}(\text{CO})_2(\text{NO})\text{L}_2$ complexes. Data were obtained in CD_2Cl_2 for L = PEt_3 (**2**), $\text{P}(\text{O}^i\text{Pr})_3$ (**3**), PPh_3 (**4**). In addition to this, data for **2** were also taken in toluene-*d*₈.

$\text{WH}(\text{CO})_2(\text{NO})(\text{PPh}_3)_2$ (**4**), the most reluctant species in terms of the adduct formation, exhibits essentially identical $\delta(\text{WH})$ with and without HFIP between -90°C and room temperature. The largest difference $\Delta\delta$ amounts to 0.03 ppm, i.e., lies within the experimental error. The chemical shifts are the same for **2** at 20°C but deviate on cooling with $\Delta\delta = 0.22$ ppm at -60 and 0.33 ppm at -90°C . A difference of 0.21–0.22 ppm is detected for **3** at -90 and -100°C .

Like the chemical shift, the $^2J(\text{H}-\text{P})$ coupling also remains unchanged when HFIP is added to **4**. Some noticeable decrease of $^2J(\text{H}-\text{P})$ is observable in the other cases. Represented as a coupling between the outermost lines, $^2J(\text{H}-\text{P})$, it amounts to 46.6/44.3 Hz (**2**) and 63.4/62.2 Hz (**3**) in the absence/presence of the alcohol.

From the data above, it follows that among the monohydrides **1–4**, $\text{WH}(\text{CO})_2(\text{NO})(\text{PPh}_3)_2$ (**4**) represents the case of the weakest interaction with HFIP. This is also reflected in the T_1 times of **4** showing small difference in the presence/absence of the alcohol. On the contrary, T_1 decreases significantly when HFIP is added to **2** and **3**. The minimum of the relaxation time, $T_{1\text{min}}$, drops from 718 to 349 ms for $\text{WH}(\text{CO})_2(\text{NO})(\text{PEt}_3)_2$ and from 700 to 460 ms for $\text{WH}(\text{CO})_2(\text{NO})[\text{P}(\text{O}^i\text{Pr})_3]_2$.

The NMR data summarized in Table 4, especially the differences in the relaxation rates ΔR_1 , show stronger interaction with HFIP in the order already established above by IR, L = $\text{PPh}_3 < \text{P}(\text{O}^i\text{Pr})_3 < \text{PEt}_3 < \text{PMe}_3$, which clearly correlates with the steric and electronic properties of the phosphines. Appar-

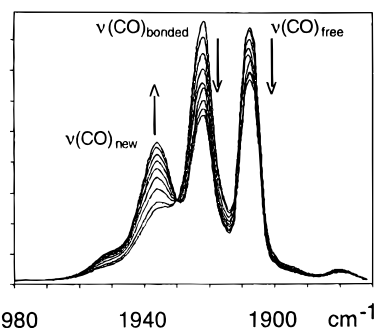


Figure 8. Intensity changes in the $\nu(\text{CO})$ range of the IR spectra following the reaction of $\text{WH}(\text{CO})_2(\text{NO})(\text{PEt}_3)_2$ with HFIP (0.004/0.03 mol/L) in hexane at 20°C . The measurements were repeated every 30 min.

ently, as exemplified by the cases of PMe_3 and PEt_3 , the steric component is important for a weak interaction when some tenths of kcal/mol may significantly change the thermodynamics.

III. Irreversible Reaction (Protonation) between the $\text{WH}(\text{CO})_2(\text{NO})\text{L}_2$ Compounds and HFIP. Complexes **1–4** are subjected to protonation by HFIP with irreversible loss of hydrogen. The rate of the reaction very much depends on the temperature, nature of the solvent, and choice of L. It is slow for all phosphorus ligands L in toluene and hexane (practically no reaction at low temperature). Hydrides **1** and **2** are quite easily protonated in CD_2Cl_2 .

The kinetic product of protonation, $[\text{W}(\text{H}_2)(\text{CO})_2(\text{NO})\text{L}_2]^+$, is apparently very unstable and cannot be detected for **1–4** even at low temperature. It is expected that substitution of the stronger π -acid nitrosyl for one CO in the known and labile²⁷ $\text{W}(\text{H}_2)(\text{CO})_3\text{L}_2$ (*trans* to the dihydrogen ligand) should reduce back-donation to the σ^* of the coordinated H_2 ligand and make the H_2 –W bond very weak in $[\text{W}(\text{H}_2)(\text{CO})_2(\text{NO})\text{L}_2]^+$.²⁸

After the loss of H_2 , the subsequent transformation did not afford $\text{W}[(\text{CF}_3)_2\text{CHO}](\text{CO})_2(\text{NO})\text{L}_2$ as an isolable product. The reaction solutions studied *in situ* by ^1H and ^{31}P NMR showed formation of at least three major species at room temperature. In the IR study (carried out in *hexane*), a new CO band (denoted as $\nu(\text{CO})_{\text{new}}$ in Figure 8 and shifted further to higher wavenumbers, 1940–1942 cm^{-1}) was observed upon protonation of **1** and **2**. The intensity of $\nu(\text{CO})_{\text{new}}$ grew slowly when those of $\nu(\text{CO})_{\text{free}}$ and $\nu(\text{CO})_{\text{bonded}}$ decreased, and an isosbestic point is clearly seen in Figure 8. The intensity of $\nu(\text{WH})$ and $\nu(\text{NO})$ of complexes **1** and **2** in these solutions decreased in a similar fashion, and one new $\nu(\text{NO})$ band of the product increased in intensity (also with isosbestic points), and shifted to higher wavenumbers. Instability of the product prevented its isolation

(27) Kubas, G. J. *Acc. Chem. Res.* **1988**, *21*, 120.

(26) Gusev, D. G.; Kuhlman, R.; Rambo, J. R.; Berke, H.; Eisenstein, O.; Caulton, K. G. *J. Am. Chem. Soc.* **1995**, *117*, 281.

(28) Burdett, J. K.; Eisenstein, O.; Jackson, S. A. In *Transition Metal Hydrides*; Dedieu, A., Ed.; VCH Publishers, Inc.: Deerfield Beach, FL 1992; Chapter 5.

and proper characterization. Comparable values of $\nu(\text{CO})$ are known²⁹ for $\text{W}(\text{OPh})(\text{CO})_2(\text{NO})[\text{P}(\text{O}^i\text{Pr})_3]_2$ (1945 cm^{-1}), $\text{W}(\text{OMe})(\text{CO})_2(\text{NO})[\text{P}(\text{O}^i\text{Pr})_3]_2$ (1956 cm^{-1}), and $\text{W}(\text{OPh})(\text{CO})_2(\text{NO})(\text{PMe}_3)_2$ (1934 cm^{-1}), indicating that the new species detected by IR might indeed be labile $\text{W}[(\text{CF}_3)_2\text{CHO}](\text{CO})_2(\text{NO})\text{L}_2$.

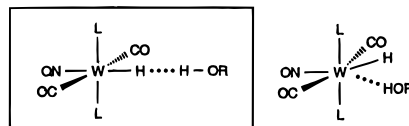
Summary of the Structural Results, Conclusion

The NMR results firmly establish that the H-bonded complex of HFIP and $\text{WH}(\text{CO})_2(\text{NO})\text{L}_2$ has close WH and OH protons. The $\text{H}\cdots\text{H}$ distance of 1.77 \AA is estimated for **I**, the adduct of **1**, and HFIP. The observation of one $\nu(\text{CO})$ IR band for the $\text{ROH}\cdots\text{HW}(\text{CO})_2(\text{NO})\text{L}_2$ complexes determines that ROH should approach the hydride in a plane bisecting the $\text{OC}-\text{W}-\text{CO}$ fragment. In consideration of the full set of structural possibilities **I-VI**, we, thus, certainly reject **V** and **VI**.

More complicated structures, which one should examine, are **II** and **III**. They show ROH in the $\text{H}-\text{W}-\text{L}$ plane with the $\text{W}-\text{H}$ bond bent toward one L to accommodate the alcohol molecule. **II** involves $\text{OH}\cdots\text{W}$ hydrogen bonding and **III** represents a case of H-bonding to two centers (the distances in the $\text{H}-\text{W}-\text{H}$ triangle seem to be comparable). A related possibility is **IV**, though it is highly questionable in view of the instability of $[\text{W}(\text{H}_2)(\text{CO})_2(\text{NO})\text{L}_2]^+$ (**IV** can be a transient species and has already been invoked to explain H/D exchange in $\text{WH}(\text{CO})_2(\text{NO})\text{L}_2/\text{CD}_3\text{OD}$ systems^{11a}).

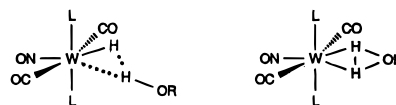
We have a number of observations against both **II** and **III**. Most significant is that **II** implies some decrease of electron density on the metal, which should cause a high-wavenumber shift of $\nu(\text{W}-\text{H})$; a low-wavenumber shift is actually reported. Structure **III** is expected to show rather fast WH/OH scrambling (via the transition structure **IV**) that is in fact not detected on the NMR time scale. Very moderate steric influence on the enthalpy of the hydrogen bonding is evident from the values of $-\Delta H^\circ$ in Table 3 ($\leq 0.03\text{ kcal/mol}$ between **1** and **2**). There is much greater dependence of $-\Delta H^\circ$ on the acidity of ROH, which is *against* the sterics: $-\Delta H^\circ$ changes from 5.2 (PhOH) to 6.9 kcal/mol (PFTB) for **1** and from 5.0 (PhOH) to 6.8 (PFTB) kcal/mol for **2**. For the formation of **II** and **III** this is unlikely. The rather close approach of ROH to the metal center, required in **II** and **III**, must be hindered when R is bulky. Structure **III** can be viewed only as a point on the reaction path that leads to transient **IV** and then to the product of complete proton transfer, the unstable $[\text{W}(\eta\text{-H}_2)(\text{CO})_2(\text{NO})\text{L}_2]^+$ compounds.

(29) (a) Kundel, P.; Berke, H. *Z. Naturforsch.* **1987**, *42b*, 993. (b) van der Zeijden, A. A. H.; Bosch, H. W.; Berke, H. *Organometallics* **1992**, *11*, 2051.



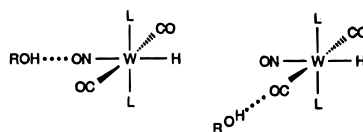
I - hydrogen bonding to H

II - hydrogen bonding to W



III - hydrogen bonding to H and W

IV - anion assisted H_2 complex



V - hydrogen bonding to NO

VI - hydrogen bonding to CO

Structure **I** represents the most reasonable molecular geometry for the hydrogen-bonded complex. It shows the symmetry required by IR around the metal center and *linear* $\text{H}\cdots\text{H}-\text{O}$ hydrogen bond, i.e., that type, which is usually considered to be the strongest. Further rearrangement in **I** to form unstable $[\text{W}(\text{H}_2)(\text{CO})_2(\text{NO})\text{L}_2]^+$ should be required to overcome a certain barrier to bring the proton closer to tungsten and break the $\text{O}-\text{H}$ bond. The latter determines the clear tendency observed for the protonation reaction to accelerate when the acidity of ROH increases.

Protonation is one of the most fundamental reactions in the chemistry of transition metal complexes. In the last 10 years it has also become a traditional route to dihydrogen complexes: when a metal hydride is protonated, coordinated H_2 is formed in the *kinetic* product.^{12,27} This synthetic evidence has always been regarded as a strong indication for the hydride ligand to be the proton accepting site. This paper presents experimental evidence for the attractive interaction that results in formation of a hydrogen-bonded $\text{ROH}\cdots\text{HW}(\text{CO})_2(\text{NO})\text{L}_2$ complex in solution prior to protonation.

Acknowledgment. We thank the Swiss National Science Foundation for financial support. The IR part of this project was supported by the International Science Foundation (grant N M6A300) and the Russian Fund for Fundamental Research (grant N93-03-45610).

JA953094Z